  Bull. Chem. Soc. Jpn., 61, 3659—3665 (1988)

Preparation and Characterization of Large Surface Area $BaO \cdot 6Al_2O_3$

Masato MACHIDA, Koichi EGUCHI, and Hiromichi ARAI*
Department of Materials Science and Technology, Graduate School of Engineering Sciences, Kyushu University, 39, Kasuga, Fukuoka 816
(Received April 4, 1988)

Barium hexaaluminate, $BaO \cdot 6Al_2O_3$, exhibited excellent heat resistance in maintaining a large surface area. Preparation from hydrolysis of metal alkoxides was a superior process in deriving the large surface area of $BaO \cdot 6Al_2O_3$, to that from mixtures of $BaCO_3/\gamma$-Al_2O_3. Direct formation of $BaO \cdot 6Al_2O_3$ phase at low temperature plays the key role in retaining the fine particle size. The amount of water added for hydrolysis and the aging period of hydrolyzed precursors strongly influenced the surface area of alkoxide-derived $BaO \cdot 6Al_2O_3$. These effects of the preparation conditions originated from the difference in microstructure and chemical structure of the hydrolyzed precursors. Monodispersed fine precursor particles with high oxide content generated large surface area $BaO \cdot 6Al_2O_3$.

Catalytic combustion has many advantages over conventional flame combustion in suppressing NO_x emission and in improving combustion efficiency. Recently, much interest has arisen in new application of this technology in gas turbines, jet engines, and boilers above 1000 °C.[1,2] In maintaining catalytic activity under such a severe condition, high heat resistance is necessary in the catalytic materials. But this is not satisfied by the catalysts at present in use for low temperature combustion. One of the crucial problems is how to suppress sintering of the oxide support in a high temperature combustion catalyst. Our research has been focused on developing a support material endowed with high heat and thermal shock resistance which also maintains a large surface area even above 1400 °C.

Alumina is one of the most common support materials used around 1000 °C. Additive oxides, such as La_2O_3, BaO, CaO, MgO, SiO_2 etc., have been reported to aid in maintaining the large surface area at elevated temperatures.[3-6] We have previously reported[7,8] that the addition of BaO greatly increases the surface area of alumina above 1000 °C. The effect of BaO depends strongly on the oxide composition. The optimum composition agrees with the stoichiometric one for the formation of $BaO \cdot 6Al_2O_3$, at which the surface area reached more than 6 $m^2 g^{-1}$ even after calcination at 1450 °C. But the improvement is still unsatisfactory in practical use for high-temperature combustion. In this paper, we report the marked elevation of high-temperature surface area retention of $BaO \cdot 6Al_2O_3$ by employing the preparation from metal alkoxides. The powder characteristics of sol-gel prepared $BaO \cdot 6Al_2O_3$ were compared with the sample from the conventional technique. It has become evident that the formation process of $BaO \cdot 6Al_2O_3$ plays a key role in the retention of large surface area.

Experimental

Sample Preparation. Barium hexaaluminate ($BaO \cdot 6Al_2O_3$) was prepared from mixtures of $BaCO_3$ (99%, Kishida Chemical) and γ-Al_2O_3 (99.9%, Catalysis Soc. Jpn., JRC-ALO4). The average crystallite size of $BaCO_3$ and γ-Al_2O_3 were 0.8 μm and 5 nm, respectively. They were mixed with an automatic mortar grinder for 2 h before firing. The mixture was heated in air at a constant rate of 5 deg min^{-1} and kept at a desired temperature for 5 h in a high-density alumina crucible.

A sample with the same composition was prepared by hydrolysis of the corresponding metal alkoxides. Barium isopropoxide, $Ba(OC_3H_7)_2$, was prepared by the reaction between Ba metal (99%, Kishida Chemical) and 2-propanol (99.5%, Kishida Chemical) in N_2 stream at 80 °C.[9]

$$Ba + 2\,C_3H_7OH \rightarrow Ba(OC_3H_7)_2 + H_2$$

Calculated amounts of $Ba(OC_3H_7)_2$ and $Al(OC_3H_7)_3$ (99%, Kishida Chemical) were dissolved together in 2-propanol and refluxed at 80 °C for 5 h with vigorous stirring. All the procedure before the hydrolysis has been carried out in a dried N_2 atmosphere. As distilled water was slowly added to the resulting solution, gelation was observed immediately accompanied by a rise in temperature from 80 to 90 °C. After several hours of aging under stirring at 80 °C, the hydrolyzed alkoxides were evaporated to dryness in vacuo and the powders thus obtained were calcined in the above mentioned manner. In this study, the surface areas of alkoxide-derived $BaO \cdot 6Al_2O_3$ were investigated as a function of the amount of water for hydrolysis and the aging period of hydrolyzed alkoxides. Thus, a series of hydrolysis reactions were performed to demonstrate these optimum conditions.

Sample Characterization. The surface areas of oxide powders were determined by the BET method using nitrogen adsorption. The surface area thus obtained was reproducible within a 10% relative error on the average. The pore size distributions were also obtained from the nitrogen adsorption isotherms at 77 K. The crystal structures of the calcined samples were determined by X-ray diffraction (Rigaku Denki, 4011). The microstructures of the powder samples were measured by a scanning electron microscope (JEOL, JSM-50).

Thermal decomposition of the hydrolyzed precursors to the corresponding oxides was observed by differential thermal analysis and thermal gravimetry (ULVAC, TGD 5000RH) in air. The samples were heated at a constant rate of 10 deg min^{-1} up to 600 °C. The infrared spectra were taken on a JASCO IR 810 spectrometer before and after the thermal decomposition. Mixtures of the hydrolyzed precursors (30 mg) and KBr powder (300 mg) were pressed into

disks of 20 mm diameter and placed in the temperature-controlled in situ cell. The infrared spectra were recorded after evacuation at elevated temperatures and subsequent cooling to room temperature.

Results

The Surface Area of $BaO \cdot 6Al_2O_3$. γ-Alumina and the two BaO-Al_2O_3 precursors, which were prepared from powder mixtures and metal alkoxides, were heated at elevated temperatures for 5 h. The decrease in surface area during the heat treatment was measured as a function of the calcination temperature (Fig. 1). The present investigation was performed only on the samples with a composition of $(BaO)_{0.14}(Al_2O_3)_{0.86}$ at which the effect of BaO on the surface area is most prominent, as has been reported previously.[7,8] The three samples in Fig. 1 had similar surface areas after calcination at 1100 °C, but the surface area significantly decreased with a rise in calcination temperature. The decrease was most significant in pure alumina. The addition of BaO was obviously effective in maintaining the surface area at higher temperatures. The effect of BaO is related to the formation of a hexagonal layered aluminate ($BaO \cdot 6Al_2O_3$).[7,8] The surface area of barium hexaaluminate prepared from $BaCO_3/\gamma$-Al_2O_3 was 4 times larger than that of pure alumina above 1300 °C.

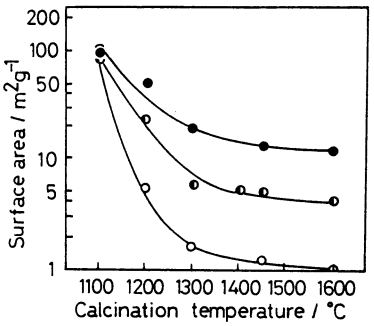

Fig. 1. Temperature dependence of surface areas of $(BaO)_{0.14}(Al_2O_3)_{0.86}$ and Al_2O_3. ● $(BaO)_{0.14}(Al_2O_3)_{0.86}$ (alkoxide), ◐ $(BaO)_{0.14}(Al_2O_3)_{0.86}$ ($BaCO_3/\gamma$-Al_2O_3), ○ Al_2O_3.

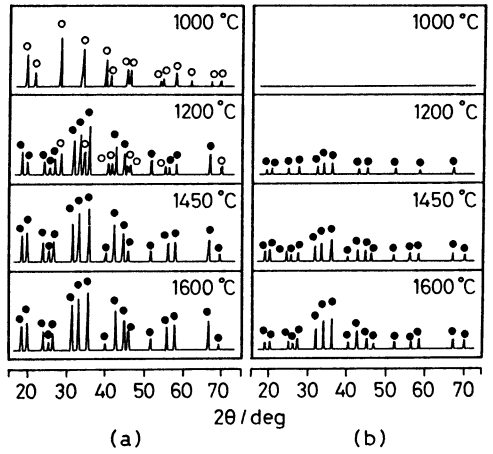

Fig. 2. X-Ray diffraction patterns of $(BaO)_{0.14}(Al_2O_3)_{0.86}$ after calcination at various temperatures. (a) Powder mixture of $BaCO_3$ and γ-Al_2O_3. (b) Hydrolyzed alkoxides. ● $BaO \cdot 6Al_2O_3$, ○ $BaO \cdot Al_2O_3$.

Preparation from alkoxide precursors, which sometimes gives rise to the formation of ultrafine particles and/or low temperature processing of mixed oxides, was applied to the present system. The data for a typical alkoxide-derived sample are shown in Fig. 1. The loss of surface area upon heating was more gradual than that of the powder mixtures. The surface area was 3 times larger than that from $BaCO_3/\gamma$-Al_2O_3 mixtures above 1300 °C.[10] The value of 11 m^2g^{-1} after heating at 1600 °C has not been achieved by any oxide supports so far reported.

The Crystal Structure of BaO-Al_2O_3. The phase diagram of the system BaO-Al_2O_3 indicates that the $(BaO)_{0.14}(Al_2O_3)_{0.86}$ sample consists of a single phase of $BaO \cdot 6Al_2O_3$ in the equilibrium state.[11] However, the $BaCO_3/\gamma$-Al_2O_3 precursor underwent a complicated formation process to evolve this phase during the heating process, as shown in Fig. 2(a). After calcination at 1000 °C, the phase observed in $BaCO_3/\gamma$-Al_2O_3 was the equimolar compound ($BaO \cdot Al_2O_3$) and a trace amount of $BaCO_3$, instead of the equilibrium phase ($BaO \cdot 6Al_2O_3$). The sample at this calcination condition is almost completely composed of a mixture of $BaO \cdot Al_2O_3$ and Al_2O_3, though the diffraction lines from the latter phase are too weak to be observed by X-ray diffraction due to its poor crystallinity. With a rise in calcination temperature, the diffraction lines from $BaO \cdot 6Al_2O_3$ appeared and became intense. The formation of the equilibrium $BaO \cdot 6Al_2O_3$ phase was completed after heating at 1450 °C.

The samples from alkoxides, on the other hand, showed no diffraction lines after heating at 1000 °C. At 1200 °C, the diffraction lines which appeared in this case were only from the $BaO \cdot 6Al_2O_3$ phase (Fig. 2(b)). They became sharp and intense at elevated calcination temperatures, but the $BaO \cdot Al_2O_3$ phase was not observed at any temperature.

Microstructures and Pore Size Distributions. After calcination at 1450 °C, the particle morphology of alumina and $BaO \cdot 6Al_2O_3$ was observed by a scanning electron microscope (SEM), as shown in Fig. 3. The particle size of alumina (ca. 2 μm) was considerably larger than that of the $BaO \cdot 6Al_2O_3$ samples. Significant grain growth of alumina is evident from the large particle size and the smooth powder surface. In contrast, the $BaO \cdot 6Al_2O_3$ powder was clearly fine and possessed a rough surface. It is noted that the two $BaO \cdot 6Al_2O_3$ samples are obviously different in their particle sizes and microstructures. When the mixture of $BaCO_3$ and γ-Al_2O_3 was calcined at 1450 °C, the resultant particles (0.5—1.0 μm) were strongly agglomerated (Fig.3(b)). Such large agglomerates were absent in the sample obtained from hydrolyzed alkoxides. The particles were in a granular shape with uni-

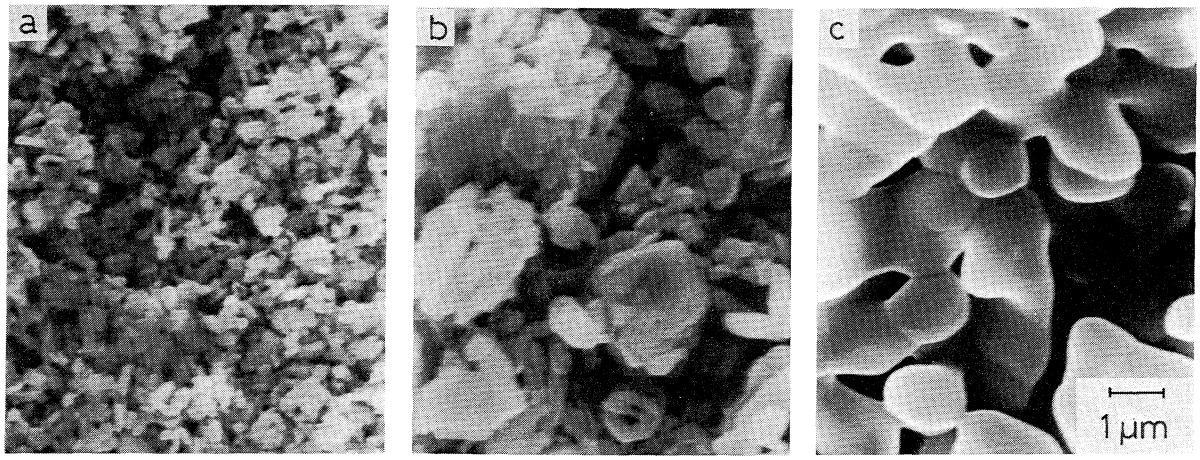

Fig. 3. SEM photographs of $BaO \cdot 6Al_2O_3$ and Al_2O_3 after calcination at 1450°C. a) $BaO \cdot 6Al_2O_3$ from alkoxides, b) $BaO \cdot 6Al_2O_3$ from $BaCO_3/\gamma\text{-}Al_2O_3$, c) Al_2O_3.

form (0.3 μm) size (Fig. 3(a)).

Pore size distributions of alumina and the $BaO \cdot 6Al_2O_3$ samples were measured after calcination at 1450 °C. The distribution was maximum at the pore size smaller than 10 nm (Fig. 4). The relative pore volume gradually decreased with increasing pore size. The barium hexaaluminate sample, in particular, that was prepared from alkoxides possessed obviously larger total pore volume than alumina. The sequence of total pore volume of three samples agreed with that of the surface area. The difference in surface area among the three alumina-based samples largely resulted from the population of pores with radius of ca. 10 nm or less.

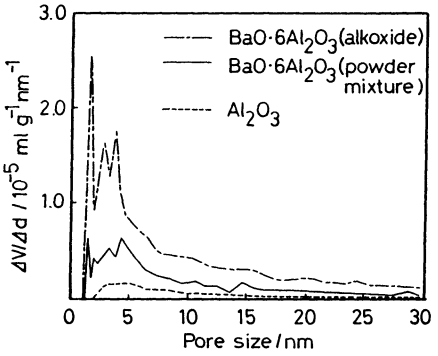

Fig. 4. Pore size distributions of $BaO \cdot 6Al_2O_3$ and Al_2O_3 after calcination at 1450°C.

Effect of Hydrolysis Conditions on Surface Area. The surface area of $BaO \cdot 6Al_2O_3$ is also sensitive to some preparation conditions during the alkoxide process such as the aging period of the hydrolyzed products and the amount of water. The surface area of alkoxide-derived $BaO \cdot 6Al_2O_3$ increased at the initial stage of aging and became almost constant after 12 h as shown in Fig. 5 ($R(H_2O/MOC_3H_7)$=10.0). After 12 h of aging and subsequent calcination at 1300 °C, the sample retained the surface area of 18.5 m^2g^{-1} which is about double that of the sample with 30 min of aging.

The amount of water added for hydrolysis is expressed as a molar ratio per metal isopropoxyl group ($R(H_2O/MOC_3H_7)$). The number of metal isopropoxyl groups, $-MOC_3H_7$, is the sum of $-AlOC_3H_7$ and $-BaOC_3H_7$. Figure 6 shows the effect of $R(H_2O/MOC_3H_7)$ on the surface area of $BaO \cdot 6Al_2O_3$. The surface area was maximum (20.2 m^2g^{-1}) at $R(H_2O/MOC_3H_7)$= 0.5, but it decreased either by an increase or by a decrease in the amount of water. The optimum condition, $R(H_2O/MOC_3H_7)$=0.5, agrees with the stoichiometric ratio for the hydrolysis of alkoxides. The effect of the amount of water is obvious especially when calcination was performed at lower temperatures such as 1300 °C.

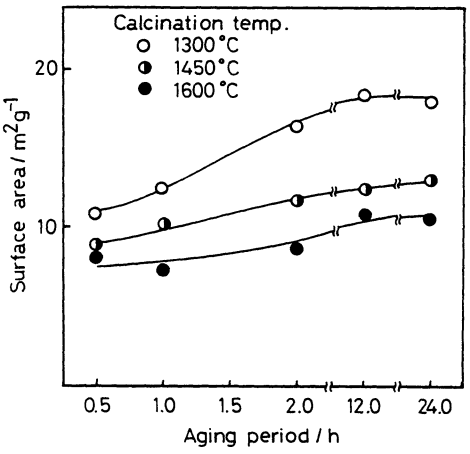

Fig. 5. Effect of the aging period of hydrolyzed precursors on the surface area of $BaO \cdot 6Al_2O_3$. ($R(H_2O/MOC_3H_7)$=10.0)

The effect of the aging period was investigated by microscopic observation of the hydrolysis precursors (Fig. 7). In the initial stage, the sample contained large agglomerates (larger than 10 μm) which consisted of submicron primary particles. With the aging progress, the size of the agglomerate was significantly reduced. After aging for 24 h, the sample consisted

almost entirely of equal sized particles and agglomerates were rarely observed.

Figure 8 shows SEM photographs of precursors after a given amount of water was added to the alkoxide solution for hydrolysis. Corresponding to the two regions observed in the surface area changes (Fig. 6), the particle morphology was different between the sample with $R(H_2O/MOC_3H_7)<0.5$ and $R(H_2O/MOC_3H_7)>0.5$. The hydrolyzed sample at $R(H_2O/MOC_3H_7)>0.5$ consisted of submicron particles, but the particle morphology and size were almost unchanged with the amount of water so far as should be observed by SEM. In contrast, the particle size was obviously larger when less water ($R(H_2O/MOC_3H_7)<0.5$) was used for hydrolysis. In this region, the amount of water is not enough for complete hydrolysis of the alkoxides. Thus, the microstructures of the hydrolysis products well reflect the surface area of the $BaO \cdot 6Al_2O_3$. Large agglomerates and large precursor particles appear to result in low surface areas after calcination.

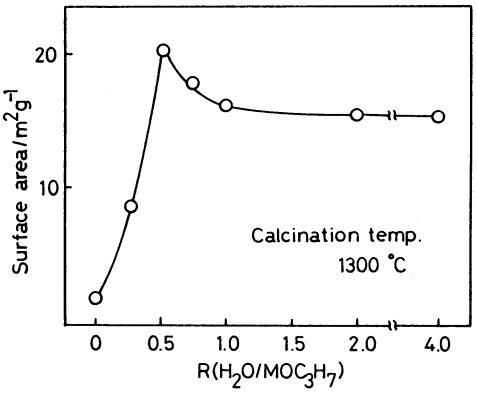

Fig. 6. Effect of the amount of water added to alkoxides on the surface area of $BaO \cdot 6Al_2O_3$. (12 h aging)

Thermal Behavior of Hydrolyzed Alkoxides. The decomposition of the hydrolyzed products was examined by in situ IR measurements. The IR spectra obtained after heating in vacuo at various temperatures are shown in Fig. 9. At room temperature, the hydrolyzed product showed the absorption band of the

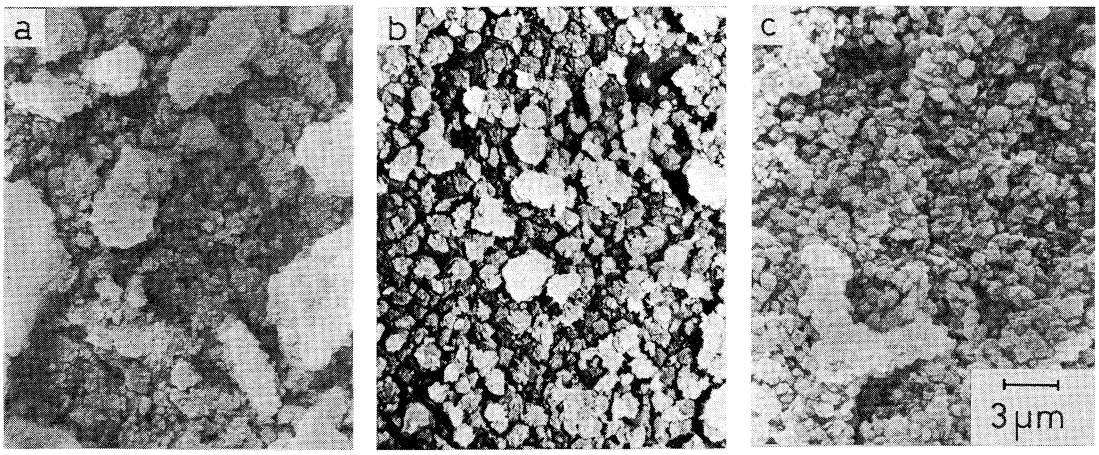

Fig. 7. Microstructures of hydrolyzed precursors with various aging period. a) 0.5 h, b) 2.0 h, c) 24.0 h. ($R(H_2O/MOC_3H_7=10.0$)

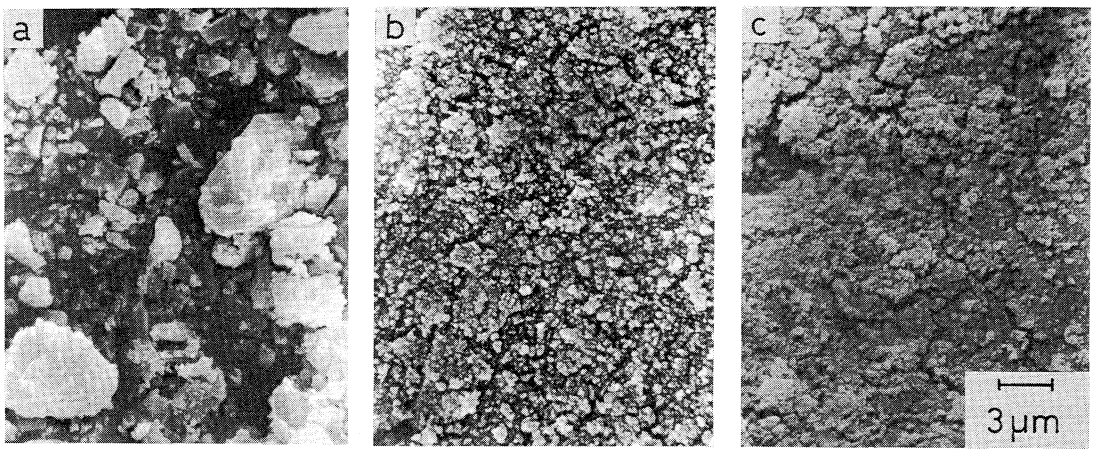

Fig. 8. Microstructures of hydrolyzed precursors with various $R(H_2O/MOC_3H_7)$. a) $R(H_2O/MOC_3H_7)=0.3$, b) 0.5, c) 1.0. (12 h aging)

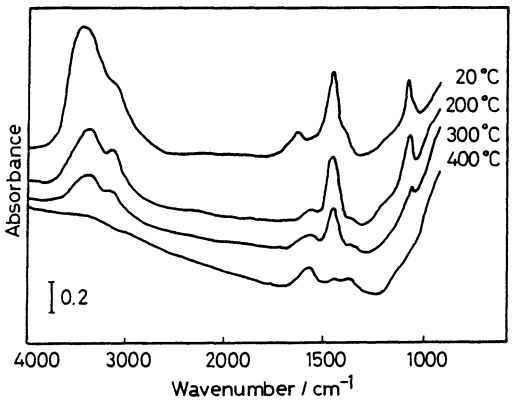

Fig. 9. Change of infrared spectrum of hydrolyzed alkoxides during the course of heating. Preparation condition of samples: $R(H_2O/MOC_3H_7)=1.0$, 12 h aging.

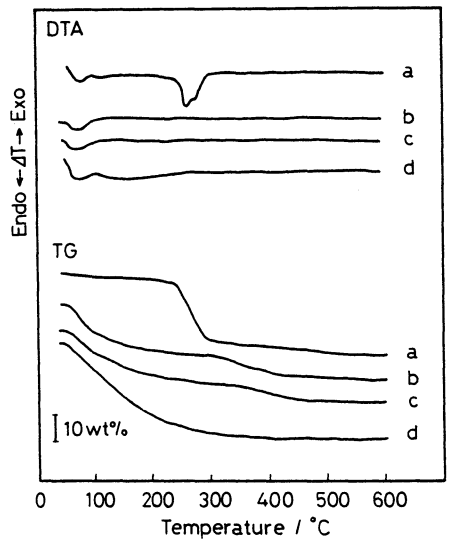

Fig. 10. DTA/TG analyses of the hydrolyzed precursors prepared under various $R(H_2O/MOC_3H_7)$ conditions. a) $R(H_2O/MOC_3H_7)=10.0$, b) 2.0, c) 1.0, d) 0.5.

H-O-H bending vibration around 1640 cm^{-1}. This band, being attributed to the physisorbed water, completely disappeared after evacuation at 200 °C. The bands at 3000—3500 cm^{-1} probably correspond to the O-H stretching mode of the metal hydroxides in the hydrolyzed precursors. These peaks were weakened at elevated temperatures due to the thermal decomposition of metal hydroxides to mixed oxides. The O-H bands disappeared at 400 °C after complete decomposition.

Figure 10 shows the DTA/TG curves of hydrolyzed precursors prepared under various $R(H_2O/MOC_3H_7)$ conditions. A broad endothermic peak below 100 °C, which was observed in every alkoxide-derived sample, is attributed to elimination of physisorbed water. A large and sharp endothermic peak with a 25% weight loss appeared for the sample with $R(H_2O/MOC_3H_7)=10$ around 250 °C. From the IR result, this weight loss can be attributed to dehydration accompanied by thermal decomposition of the metal hydroxides. Similar weight loss was observed in the samples with $R(H_2O/MOC_3H_7)<2.0$ at 250—400 °C, but they were small, corresponding to the small content of metal hydroxides.

Discussion

Effect of $BaO \cdot 6Al_2O_3$ Formation on Surface Area. Although a large surface area is one of the most important properties for combustion catalysts, only little is known about the support material for high-temperature combustion. Most support materials, which have been used so far below 1000 °C, sinter into particles with only a small surface area. γ-Alumina, which is most commonly used as a catalyst support below 1000 °C, is not adequate because of its significant decrease in surface area, as shown in Fig. 1. The decrease in the surface area around 1200 °C is accompanied by a phase transition from metastable states into the equilibrium phase (α-phase). In contrast, BaO added alumina is effective in maintaining the large surface area by forming the $BaO \cdot 6Al_2O_3$ phase.

The structure of $BaO \cdot 6Al_2O_3$ has been described as the intermediate of magnetoplumbite and β-alumina structures (Fig. 11).[12,13] But the detailed refinement of the crystal structure with this composition reported by Kimura et al.[14,15] revealed the existence of two compounds near the stoichiometric $BaO \cdot 6Al_2O_3$ composition. It was suggested that they are essentially β-alumina structures on the basis of the electron diffraction and crystallographic data. Both the magnetoplumbite and β-alumina structures are grouped into a layered aluminate type, but they differ from each other in the atomic arrangement in the mirror plane. In our previous reference on a series of alkaline earth oxide-alumina systems,[8] the aluminate samples which crystallize in the layered aluminate structures generally possessed the large surface area. It was also reported[16] that some rare earth metal aluminates with these layered structures exhibited large surface areas after heating at high temperatures. However, the $BaO \cdot 6Al_2O_3$ system is the most prominent in main-

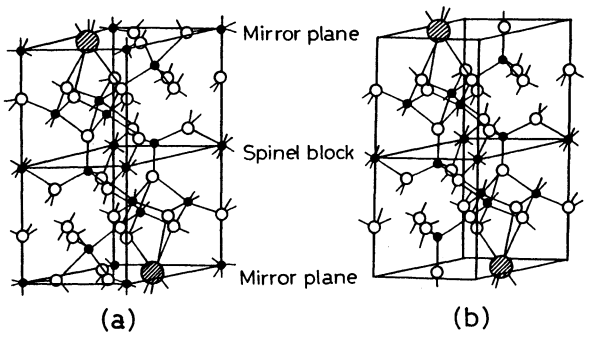

Fig. 11. Crystal structure of (a) magnetoplumbite and (b) β-alumina. ● Al^{3+}, ○ O^{2-}, ● Ba^{2+}.

taining the large surface area among the series of layered aluminates with large di- or trivalent cations. The real reason for such high thermal resistance against sintering is not sufficiently understood at present, but it is probably related to the crystal structure. In the layered aluminate structure, each layer is separated by the mirror plane (Fig. 11). The structure may suppress interlayer diffusion of atoms and crystal growth along the *c* direction (perpendicular to the mirror plane). In fact, polycrystalline sodium β-alumina, which is used as a solid electrolyte, grows as plate-shaped particles with their flat sides perpendicular to the *c* axis. Powers et al.[17] suggested that the stacking of layers in sodium β-alumina is very slow in comparison to the Al-O spinel formation. It was deduced that the mirror planes, which separate each spinel block, seem to play a key role in the large surface area of the layered aluminate family.

Effect of Preparation Procedure of $BaO \cdot 6Al_2O_3$. There are some superior points of an alkoxide process as compared with a conventional method, i.e., 1. high purity, 2. very fine primary particle, and 3. uniform mixing of components.[18,19] The first factor seems not to be so important for the high surface area of the system, because small amount of additives, such as Cr, Mn, and Co did not promote sintering.[20] Particles are desired to be fine to obtain a large surface area, but ultrafine particles are apt to sinter due to their large surface energy. At present, the third point is expected to be the most important in achieving the large surface area of $BaO \cdot 6Al_2O_3$. As mentioned above, the formation of barium hexaaluminate is essential for the large surface area of the present system. The alkoxide process permits direct formation of this phase by uniform mixing of the components at a molecular level (Fig. 2). To make a comparison with hydrolysis of the alkoxide mixture, barium isopropoxide and aluminium isopropoxide were separately hydrolyzed in 2-propanol solutions and the resulting hydroxide suspensions were mixed and evaporated to dryness. The phases appearing after calcination at 1300 °C were not only $BaO \cdot 6Al_2O_3$ but also $BaO \cdot Al_2O_3$. This indicates that high chemical homogeneity is attained only when a mixture of the two alkoxides is hydrolyzed simultaneously. In other words, the mixing at a particle level does not reduce the formation temperature of $BaO \cdot 6Al_2O_3$. It is likely that the mixing of the two alkoxides in 2-propanol leads to formation of mixed alkoxides;[21] but direct evidence for the formation of mixed alkoxides has not been obtained. The high chemical homogeneity in the alcoholic solution should be retained in alkoxide-derived precursors as a consequence of solution gelation.

On the other hand, in the case of powder mixtures, barium hexaaluminate is formed through the solid state reaction between $BaO \cdot Al_2O_3$ and alumina by diffusion. Since the excellent heat resistance is not achieved by the $BaO \cdot Al_2O_3$ phase, the $BaO \cdot Al_2O_3$ particles grow in size during the solid state reaction until they are converted to $BaO \cdot 6Al_2O_3$. Thus, it is concluded that the high surface area of the alkoxide-derived sample is a result of the low temperature formation of $BaO \cdot 6Al_2O_3$.

The difference in the reaction history is well reflected in the microstructures of the powders. The SEM photographs demonstrated a marked contrast in microstructure of the two barium hexaaluminate samples (Fig. 3). Although large agglomerates and unequal particle size are observed commonly in the powder mixtures, the alkoxide-derived samples consist of submicron particles with a uniform size. The difference in microstructure is reflected by the pore size distribution. Large primary particles in the powder mixture result in small overall pore volume as shown in Fig. 4. The pores smaller than 10 nm in diameter largely contribute to the difference in the total pore volume of the three samples. Pores of this size are in fact seen in the SEM photograph of the alkoxide-derived $BaO \cdot 6Al_2O_3$ sample as interparticle voids.

Effect of Preparation Condition in Alkoxide Process. The surface areas of samples from the alkoxide process were affected by the amount of water and the aging period after hydrolysis. The change in surface area with the amount of water is apparently divided into two regions as shown in Fig. 6. The stoichiometric amount of water for the decomposition of alkoxides is $R(H_2O/MOC_3H_7) = 0.5$.

$$2\text{-M-}(OC_3H_7) + H_2O \rightarrow \text{-M-O-M-} + 2\,C_3H_7OH \quad (1)$$

At $R(H_2O/MOC_3H_7) < 0.5$, the oxide is produced partly by hydrolysis (Reaction(1)) and partly by pyrolysis of the alkoxides. The increase in surface area in this region indicates that pyrolysis of the alkoxides does not contribute to the large surface area. Namely, a substantial amount of hydrolysis is required to produce a large surface area. The particle size of the incompletely hydrolyzed product is two orders of magnitude larger than that of the sample at $R(H_2O/MOC_3H_7) > 0.5$ (Fig. 8).

At the second region ($R(H_2O/MOC_3H_7) > 0.5$), the surface area decreases with an increase in $R(H_2O/MOC_3H_7)$ (Fig. 6). The partial formation of hydroxides (Reaction(2)) is included, due to the presence of excessive water in this region.[22]

$$M(OC_3H_7)_n + nH_2O \rightarrow M(OH)_n + nC_3H_7OH \quad (2)$$

As the amount of water increases, the reaction (2) becomes dominant, resulting in a high content of hydroxide groups in the product. The hydroxides thus formed are thermally decomposed into oxides accompanying elimination of water in the temperature range 250—400 °C as was observed by TG. The weight loss in this temperature range increased with $R(H_2O/MOC_3H_7)$, corresponding to the increase in the hydroxide content in the precursors. The formation temperature of $BaO \cdot 6Al_2O_3$ for the sample with a low

extent of hydrolysis ($R(H_2O/MOC_3H_7)<1.0$) was near 1100 °C, while it is above 1200 °C for the hydroxide-rich sample ($R(H_2O/MOC_3H_7)=10.0$). The decrease in surface area in the second region resulted from the hydroxide formation in precursors. This also elevates the temperature for the formation of $BaO \cdot 6Al_2O_3$

The effect of the aging period in Fig. 5 is somewhat smaller than that of the amount of water. The increase in surface area with aging is related to the extent of agglomeration of hydrolyzed products as was revealed by SEM observation in Fig. 7. The aging of hydrolyzed products in the presence of excessive water likely reduces the agglomeration of particles and brings about a high dispersion state. Large agglomerates, which are observed at a short aging period, grow into large particles in the course of heating. This only leads to the decrease in the surface area of the resultant $BaO \cdot 6Al_2O_3$

The authors are greatly indebted to the Center of Advanced Instrumental Analysis of Kyushu University for support in SEM measurements. This research was partially supported by a Grant-in-Aid for Scientific Research No. 61550598 from the Ministry of Education.

References

1) D. L. Trimm, *Appl. Catal.*, **7**, 249 (1983).
2) R. Prasad, L. A. Kennedy, and E. Ruckenstein, *Catal. Rev.*, **26**, 1 (1984).
3) I. Amato, D. Martorama, and B. Silengo, "Sintering and Catalysis," ed by G. C. Kuczynski, Plenum Press, New York and London (1975), p. 187.
4) H. Schaper, E. B. M. Doesburg, and L. L. Van Reijen, *Appl. Catal.*, **7**, 211 (1983).
5) H. Schaper, E. B. M. Doesburg, P. H. M. De Korte, and L. L. Van Reijen, *Solid State Ionics*, **16**, 261 (1985).
6) R. M. Levy and D. J. Bauer, *J. Catal.*, **9**, 76 (1967).
7) M. Machida, K. Eguchi, and H. Arai, *Chem. Lett.*, **1986**, 151.
8) M. Machida, K. Eguchi, and H. Arai, *J. Catal.*, **103**, 385 (1987).
9) K. S. Mazdiyansni, R. Dolloff, and J. S. Smith II, *J. Am. Ceram. Soc.*, **52**, 523 (1969).
10) M. Machida, K. Eguchi, and H. Arai, *Chem. Lett.*, **1986**, 1993.
11) E. M. Levin, C. R. Robbines, and H. F. McMurdie, "Phase Diagrams for Ceramists," Fig. 206. Am. Ceram. Soc. Columbus, (1964).
12) J. M. P. J. Verstegen and A. L. N. Stevels, *J. Lumin.*, **9**, 406 (1974).
13) A. L. N. Stevels and A. D. M. Schrama-de Pauw, *J. Electrochem.*, **123**, 691 (1976).
14) S. Kimura, E. Bannai, and I. Shindo, *Mat. Res. Bull.*, **17**, 209 (1982).
15) N. Iyi, S. Takekawa, Y. Bando, and S. Kimura, *J. Solid State Chem.*, **47**, 34 (1983).
16) H. Yamashita, A. Kato, N. Watanabe, and S. Matsuda, *Nippon Kagaku Kaishi*, **1986**, 1169.
17) R. W. Powers and S. P. Mitoff, "Solid Electrolytes," ed by P. Hagenmuller and W. Van Gool, Academic Press, New York (1978), pp. 123—144.
18) B. Yoldas, *Am. Ceram. Soc. Bull.*, **54**, 289 (1975).
19) D. W. Johnson, Jr., *Am. Ceram. Soc. Bull.*, **64**, 1597 (1985).
20) M. Machida, K. Eguchi, and H. Arai, *Chem. Lett.*, **1987**, 767.
21) D. C. Bradly, R. C. Mehrotra, and D. P. Gaur, "Metal Alkoxides," Academic Press, New York (1978), p. 199.
22) B. E. Yoldas, *J. Am. Ceram. Soc.*, **65**, 387 (1982).